Optomechanical temporal sampling of terahertz signals

Baptiste Chomet, Djamal Gacemi, Angela Vasanelli, Carlo Sirtori, Yanko Todorov

Applied Physics Letters

Optomechanical temporal sampling of terahertz signals

Cite as: Appl. Phys. Lett. **119**, 181103 (2021); https://doi.org/10.1063/5.0068852
Submitted: 27 August 2021 • Accepted: 30 September 2021 • Published Online: 01 November 2021

Baptiste Chomet, Djamal Gacemi, Angela Vasanelli, et al.

Applied Physics Letters ARTICLE scitation.org/journal/apl

Optomechanical temporal sampling of terahertz signals

Cite as: Appl. Phys. Lett. **119**, 181103 (2021); doi: 10.1063/5.0068852
Submitted: 27 August 2021 · Accepted: 30 September 2021 ·
Published Online: 1 November 2021

Baptiste Chomet, Djamal Gacemi, Angela Vasanelli, Carlo Sirtori, and Yanko Todorov[a]

AFFILIATIONS

Laboratoire de Physique de l'Ecole Normale Supérieure, ENS, Université PSL, CNRS, Sorbonne Université, Université de Paris, Paris, France

[a]Author to whom correspondence should be addressed: yanko.todorov@phys.ens.fr

ABSTRACT

Various detection schemes are currently investigated in the terahertz frequency range (<2 THz), as an alternative to the widespread bolometers and Golay cells that feature very high sensitivity but low modulation frequencies (<10 kHz). In this work, we report an alternative concept based on an optomechanical detector able to read out an arbitrary periodic modulation imprinted on a terahertz beam. The detector is a based on a combination of a split-ring resonator, acting as a terahertz antenna, and a high-quality mechanical resonator with typical resonant frequency $\omega_0/2\pi = 1$ MHz. We demonstrate two methods for Fourier sampling the envelope of the terahertz signal, in which the mechanical resonator is used as a reference oscillator. With our methods, signals with an arbitrary period T can be sampled, even those that are much faster than the oscillation period of the mechanical resonator, $1/T \gg \omega_0$.

The terahertz frequency range (1–10 THz) of the electromagnetic spectrum is currently a playground of intense research.[1,2] There are many potential applications such as imaging, high speed communication, and noninvasive diagnosis of materials and thin films.[1–3] Those applications call for suitable detection technologies that rely on compact, sensitive, and possibly room temperature detectors. For frequencies above 2 THz, bolometric and pyroelectric detectors are currently extremely widespread. Being very sensitive (noise equivalent power $\sim$pW/Hz$^{0.5}$), helium cooled Si or Ge bolometers are still the best solution, even though they are extremely slow (typical modulation bandwidth < 100 Hz).[4] Therefore, in recent decades, there has been an important research effort to provide THz detectors that are viable alternative to bolometers: THz quantum well infrared detectors,[5,6] Schottky diodes,[7] semiconductor nanowires,[8] graphene-based plasmon detectors,[9] as well as optomechanical detectors[10–13] to cite a few. The emerging optomechanical detectors appear as an interesting solution as they can be very compact, relatively fast (10 kHz to few MHz bandwidths) and can operate at room temperature.

We recently proposed a THz detector concept based on high quality factor mechanical nano-oscillators with a typical resonance in the MHz range, in which a modulated THz field acts as an external force on the oscillator.[10,13] Typically, very high mechanical quality factors are required in order to achieve high responsivity. Therefore, incoming THz radiation must be modulated at a frequency ω_0, which ideally matches the mechanical resonance. It, therefore, appears that the ability of this highly resonant detector to follow the temporal evolution of a complex THz signal, composed of several different Fourier components, is limited. In this paper, we show that this limitation can be lifted, and arbitrary periodic signals can be sampled. In our approach, inspired from RF lock-in amplifier techniques,[14] the high-quality factor of the mechanical resonator becomes an asset instead of a drawback. Furthermore, we show that signals with an arbitrary period T can be sampled, even those that are much faster than the oscillation period of the mechanical resonator, $1/T \gg \omega_0$. This technique, therefore, overcomes the limitation of other methods demonstrated so far, such as those based on frequency phased locked loops,[11] where the detection bandwidth is limited between 0 and $1/\tau$, where τ is a photothermal response time that is typically $\tau \sim 20/\omega_0$.[15]

The device architecture employed in these studies is recalled in Fig. 1(a). The mechanical oscillator is a nanocantilever that is integrated into a rectangular split-ring resonator (SRR) with a fundamental resonance at 2.7 THz.[10] The lowest frequency modes of the nanocantilever are two flexural modes around 1 MHz, vibrating, respectively, in the plane and out of the plane of the device.[10] The nanocantilever is set in motion by illuminating the SRR with a THz wave, which excites resonantly the electromagnetic mode of the system. For this work, we exploit the out-of-plane mode, vibrating at 1.2 MHz, which is excited by a photothermal mechanism that provides

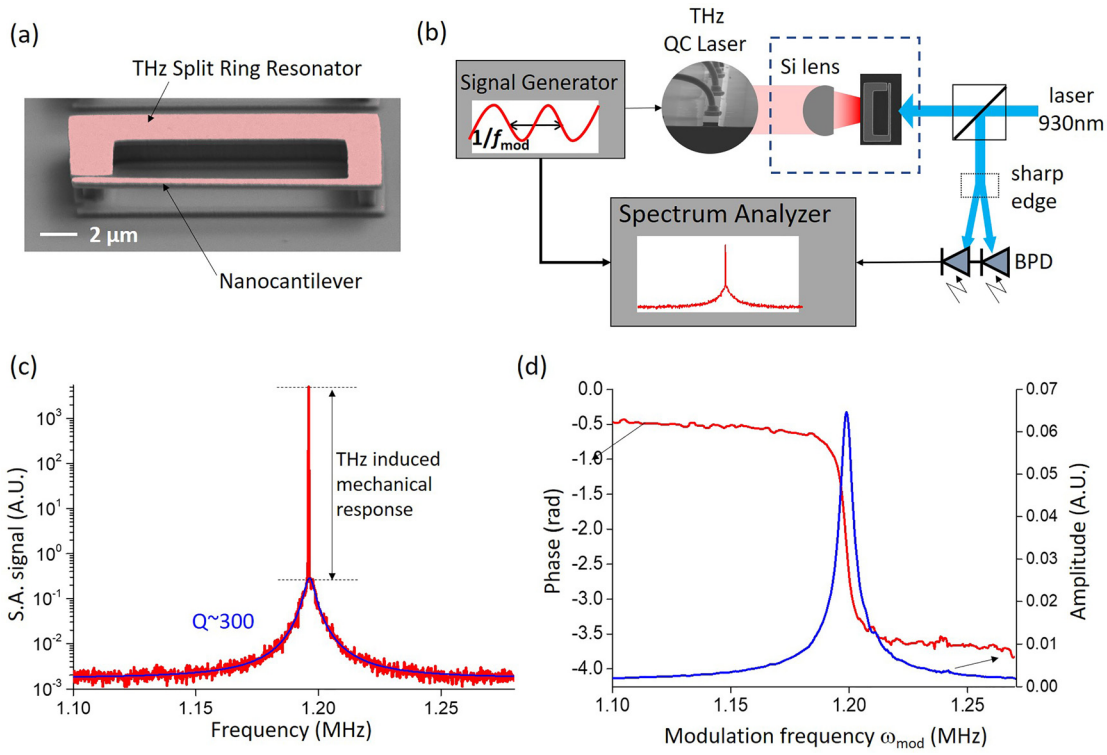

FIG. 1. (a) Scanning electron microscope picture of the optomechanical detector. (b) Schematics of the setup used to excite and probe the mechanical response of the split-ring coupled nanocantilever. (c) Output of the spectrum analyzer (see 1(b)), which shows the Brownian motion of the nanocantilever as well as the response induced by modulation of the THz laser beam. A fit of the Brownian motion spectrum allows determining a quality factor $Q = 300$ for the mechanical resonance. (d) Response obtained by scanning the frequency of the THz envelope. The spectrum analyzer is at the zero-scan mode, while its internal clock is set to the frequency of the nanobeam.

the highest response.[10] As shown in Fig. 1(b), the source of THz radiation is a quantum cascade laser. The mechanical movement of the cantilever is read out with an optical setup, using a 930 nm laser that is focused on the cantilever. Part of the laser beam is reflected from the cantilever and sent to a balanced photodetector (BPD) unit through a sharp edge mirror. In this configuration, the sensitivity of the system allows us to measure the cantilever displacement when it is only limited by the 300 K Brownian motion.[10] The latter is clearly visible in the RF spectrum of the BPD signal, which is measured using a spectrum analyzer as shown in Fig. 1(c). From the Brownian motion spectrum, it is possible to accurately measure the frequency and linewidth of the mechanical resonance, as well as to calibrate the absolute value of the mechanical displacement.[10,16] To observe the THz induced force, we apply a sine modulation on the driving QCL current with a modulation frequency ω_{mod} close to the mechanical resonance of the cantilever. The THz induced signal then appears as a delta-like peak on top of the Brownian spectrum [Fig. 1(c)]. When the modulation frequency ω_{mod} is swept in the RF range around the resonance ω_0, we can also plot the amplitude and phase of the THz mechanical response, as shown in Fig. 1(d). For this purpose, the BPD signal is fed in a lock-in amplifier that is locked to ω_{mod}. As seen from Fig. 1(d), the amplitude of the displacement follows the bandpass filter form, expected for a driven oscillator: $|z(\omega_{mod})| = |z_0\omega_0^2/(\omega_0^2 - \omega_{mod}^2 + i\omega_0\omega_{mod}/Q)|$ ($Q \sim 300$ is the mechanical quality factor), while the phase of the signal undergoes a π jump as the modulation frequency ω_{mod} crosses the resonant frequency ω_0 (here, z_0 is the static displacement of the resonator, $\omega_{mod} \to 0$).

We are first going to show how this system can sample signals with the fundamental frequencies ω_{mod} between 0 and ω_0. The signal is written as an amplitude modulation on the THz beam and then sent to the SRR-coupled nano-cantilever. Our method allows us to extract both the amplitude and phase of the Fourier components of the periodic signal written on the incoming THz wave. Let us consider a very general situation, where the modulated signal is an arbitrary time-periodic function $S(t)$ such as $S(t+T_m) = S(t)$. We can express the signal as a Fourier series in a complex notation

$$S(t) = \sum_n S_n \exp(in\omega_{mod}t). \tag{1}$$

Because $S(t)$ is a real signal, we have $S_n = S_{-n}{}^*$, and therefore, it is sufficient to consider only positive values of n. The THz signal induces a photothermal force,[10] and the equation of motion of the cantilever is that of a driven harmonic oscillator subject to a retarded force[15]

$$\ddot{z} + \dot{z}\left(\frac{\omega_0}{Q}\right) + z\omega_0^2 = \int_{-\infty}^{t} S(t')e^{-\frac{t-t'}{\tau}}dt'/\tau. \tag{2}$$

Here, τ is the heat diffusion time.

In our experiments, we measure the mechanical displacement of the cantilever with the help of a spectrum analyzer in the zero scan

mode, where the internal clock frequency is set on the mechanical resonance of the cantilever, ω_0 and, therefore, allows the measurements of the two quadratures of the mechanical movement

$$R = 1/T_0 \int_0^{T_0} z(t)\cos(\omega_0 t)dt, \quad I = 1/T_0 \int_0^{T_0} z(t)\sin(\omega_0 t)dt. \quad (3)$$

Here, $T_0 = 2\pi/\omega_0$. Using decomposition (1) and solving Eq. (2) for periodic excitation, we obtain the following expressions for the quadratures defined in (3)

$$R(x) = \frac{1}{\pi\omega_0^2}\sum_{n>0} Re\left\{T(y_n)S_n e^{i\pi y_n}\right\}(-1)^n \frac{y_n \sin(\pi y_n)}{y_n^2 - 1}, \quad (4)$$

$$I(x) = -\frac{1}{\pi\omega_0^2}\sum_{n>0} Im\left\{T(y_n)S_n e^{i\pi y_n}\right\}(-1)^n \frac{\sin(\pi y_n)}{y_n^2 - 1}, \quad (5)$$

$$T(y_n) = \frac{1}{1 - y_n^2 + iy_n/Q} \times \frac{1}{1 + i\beta y_n}. \quad (6)$$

In the above equations, the variable x is defined as $x = \omega_0/\omega_{\mathrm{mod}}$ and the variable $y_n = n\omega_{mod}/\omega_0 = n/x$. The quantity $T(y_n)$ defined in Eq. (6) arises from the response function of the harmonic oscillator: the first term on the right hand side is related to the transmission function $1/(\omega_0^2 - \omega^2 + i\omega_0\omega/Q)$, while the second arises from the retardation factor $1/(1 + i\omega\tau)$, which is the Fourier image of the exponential function in Eq. (2). In Eq. (6), we have defined $\beta = \omega_0\tau$, where $\beta = 20.5$ for our particular device. These equations are valid also in the case where the cantilever is excited by an instantaneous force such as the Coulomb force;[13] it is sufficient to set the photothermal time to zero in the above expression, $\tau = 0$ ($\beta = 0$).

The spectrum analyzer provides us with the amplitude $A(x) = (R^2 + I^2)^{1/2}$ and the phase $\phi(x) = a\tan(I/R)$ of the mechanical oscillations. By varying the modulation frequency ω_{mod}, we can plot the functions $A(x)$ and $\phi(x)$ for any type of the periodic signal $S(t)$. As a first example, as depicted in Fig. 2, we consider a THz envelope that is a pulse train with a duty cycle of 2%. The profile S(t) was obtained by a standard function generator and was superimposed with a constant component of the driving current, which does not play any role for the following discussion. We perform the same experiment described in Fig. 1(d), while the modulation frequency ω_{mod} is varied around ω_0. Instead of a single peak at ω_0, we now observe series of peaks in the amplitude mechanical response, Fig. 2(a). To relate this observation with the above model, the amplitude is retraced as a function of the variable $x = \omega_0/\omega_{\mathrm{mod}}$. The peaks now appear regularly spaced for $x = n$. From expressions (4)–(6), it is straightforward to show that the amplitudes $A(x = \mathrm{n})$ are proportional to the Fourier components $|S_n|$ of the periodic signal. In particular, in Fig. 2(b), we observe that the amplitude of the peaks vanishes around $n = 50$ and $n = 100$, as expected for a square pulse wave, where $S_n = \sin(nf\pi)/n$ with a duty cycle $f = 0.02$. Notably, a total of $n_{\max} = 106$ Fourier harmonics have been scanned in this experiment.

Our Fourier reconstruction can be understood intuitively as follows. The condition $x = n$ is equivalent to $n\omega_{\mathrm{mod}} = \omega_0$, that is, the n-th Fourier harmonic of the signal, $S_n e^{in\omega_{mod}t}$, matches the resonant oscillation frequency of the cantilever, ω_0. The mechanical response is then dominated by the response to the excitation, $S_n e^{in\omega_{mod}t}$; all other Fourier components are filtered out by the passband transmission function of the oscillator. Similarly, the phase of the n-th Fourier harmonics, ϕ(x), can also be retrieved (not shown). In summary, by scanning the modulation frequency ω_{mod} of an arbitrary periodic signal $S(t)$ and measuring the corresponding amplitude A(x) and phase functions ϕ(x), we can determine the amplitude and the phase of each of its Fourier component S_n; this allows the reconstruction of signals through Eq. (1). In Fig. 2(c), we show the corresponding reconstruction of the pulse train from the data. The temporal shape is compared with the shape that is obtained from the analytical formula by summing up to $n_{\max} = 106$ Fourier harmonics. In both cases, we apply a Lancsoz factors correction.[17] Very good correspondence is observed between the data and the expected Fourier reconstruction.

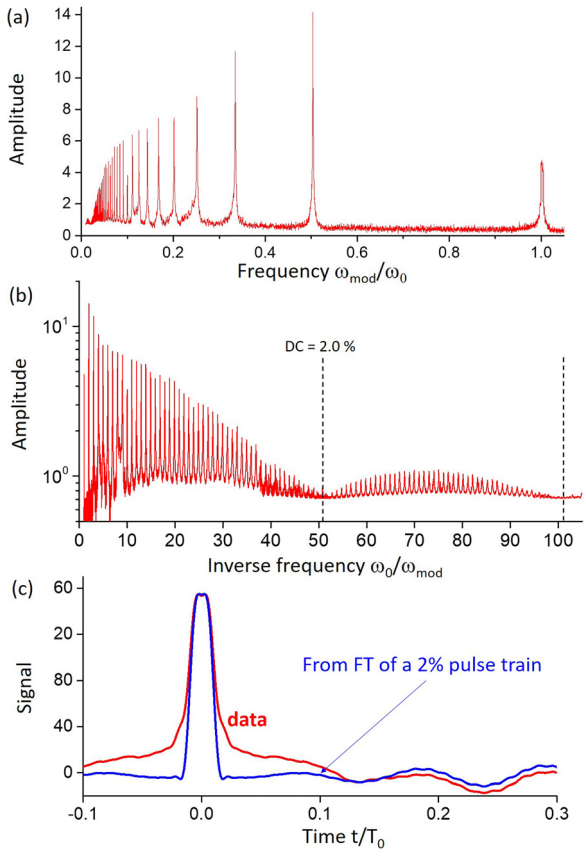

FIG. 2. (a) Mechanical response induced by a THz modulation envelope in the form of a 2% pulse train. The fundamental frequency of the signal, ω_{mod}, is swept from ω_0 to 0, where ω_0 is the resonant frequency of the nanobeam. (b) Same data as in (a) plotted as a function of the inverse frequency ratio $\omega_0/\omega_{\mathrm{mod}}$. "DC = 2%" indicates the expected ratio $\omega_0/\omega_{\mathrm{mod}}$ where the peak amplitude becomes zero for a pulse train with a 2% duty cycle. (c) Temporal profile of the THz envelope reconstructed from the data. The experimental curve is compared to a model based on the Fourier series that uses the same number of Fourier harmonics and their analytical expressions for a 2% pulse train.

We have further examined a 25% duty cycle square wave and a sawtooth signal, Figs. 3 and 4. In Figs. 3(a) and 3(b), we provide the corresponding measurements of the amplitude $A(x)$ already transformed for the $x = \omega_0/\omega_{\mathrm{mod}}$ axis. The measurements are compared with the model based on Eqs. (3)–(6). For these measurements, up to 32 harmonics for each signal were recorded. The square wave is

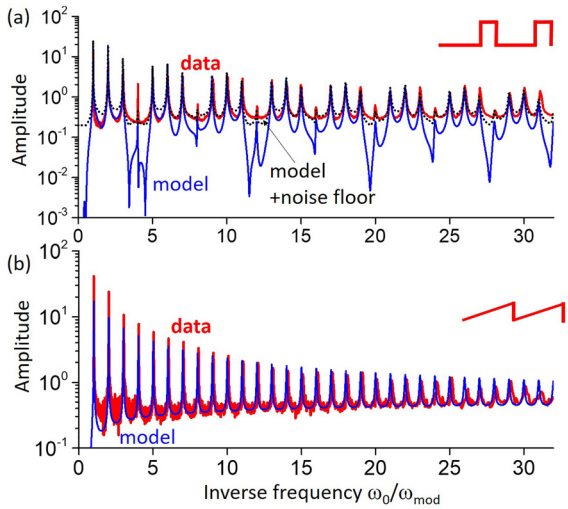

FIG. 3. Mechanical response acquired under the same conditions as Fig. 2(a), where the THz envelope is a 25% duty cycle square wave (a) and a sawtooth wave (b). Data are compared with models described in the main text.

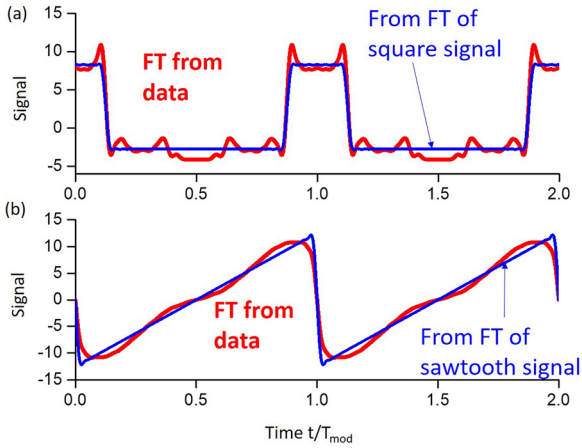

FIG. 4. Temporal reconstruction of the 25% square wave (a) and the sawtooth wave (b). The reconstructed signals are compared with the ones expected form the analytical expressions of the Fourier harmonics, using the same number of harmonics as in the experiments.

modeled with $S_n = \sin(nf\pi)/n$, with f = 0.252, while for the sawtooth wave, we have $S_n = \mathrm{i}(-1)^n/n$. We have also recorded the phase $\phi(\mathrm{x})$ for both signals; as they are real and either odd or even, the phase $\phi(\mathrm{x})$ has only π shift at $x = \mathrm{n}$ arising from the transfer function $T_\mathrm{n}(\mathrm{x})$ (not shown).

First, let us consider the 25% square wave [Fig. 3(a)]. In the case of a perfect 25% signal, every fourth harmonics is zero. We, however, observe a non-zero residual signal: this effect can be modeled by considering slightly a higher filling factor of 25.2%. The model also predicts very sharp minima around every fourth harmonics. These are actually not observed in our experiment because of the noise floor of the spectrum analyzer. A good agreement with the experimental amplitude is observed by adding a constant contribution to the amplitude $A(\mathrm{x})$ in order to model the noise floor. For the sawtooth signal, Fig. 3(b), excellent match is observed without the need of a noise floor contribution.

Using the experimental results in Fig. 3, we have extracted the amplitudes for each peak, obtaining, thus, an experimental evaluation of the Fourier amplitudes $\mathrm{S_n}$. The temporal shape of the signal $S(\mathrm{t})$ has been reconstructed in Fig. 4 using (1) and Lanczos factors.[17] The data are compared with reconstruction with $n_{\max} = 32$ harmonics using the analytical expressions $S_n = \sin(nf\pi)/n$ [Fig. 4(a)] and $S_n = \mathrm{i}(-1)^n/n$ [Fig. 4(b)]. Good agreement with the expected shapes is observed, apart from some residual oscillations in the experimental data. Our method, thus, clearly renders the temporal shape of the THz modulation.

The set-back of the approach discussed so far comes from the necessity to vary the modulation frequency of the signal ω_{mod} between 0 and ω_0. In practice, one is rather interested in measuring an envelope with a fixed frequency ω_{mod}. Therefore, we have generalized our approach in order to achieve such measurements, as described in Fig. 5(a). We assume that the waveshape to be determined is imprinted on the THz QCL laser beam with a fixed ω_{mod}. Before reaching the mechanical oscillator, the beam is passed through an intensity modulator, driven by an RF input $\cos(\omega_{sweep}t)$, where the frequency ω_{sweep} can be varied. The output of the system is then of the form $S(t)\mathrm{x}(1 + \varepsilon\cos(\omega_{\mathrm{sweep}}t))$. Using the same derivation as described above, we find that the optomechanical response of the system is still provided in Eqs. (3)–(6) if the variable y_n is defined as $y_\mathrm{n} = (\omega_{\mathrm{sweep}} - n\omega_{\mathrm{mod}})/\omega_0$. Now the peaks that correspond to the n-th Fourier component appear for the condition $\omega_{sweep} = n\omega_{\mathrm{mod}} + \omega_0$. To test this idea, we performed an experiment where the modulation, $\cos(\omega_{\mathrm{sweep}}t)$, is synthetized directly in the current driving the QCL. For our demonstration, we set $S(t)$ as a pulse train of squared pulses with 20% duty cycle and a fundamental frequency $\omega_{\mathrm{mod}} = 1$ MHz, while ω_{sweep} was varied from 2 to 13 MHz. To reduce the acquisition time, we scanned only frequency intervals of 100 kHz, where the Fourier peaks are expected to occur. The experimental results are shown in Fig. 5(b). In Fig. 5(c), we have plotted the Fourier amplitudes extracted from the data in Fig. 5(b), and we have compared them with the analytical expression $S_n = \sin(nf\pi)/n$ with $f = 0.2$. Finally, in Fig. 5(d) we plot the signal temporal shape of the experimental data in comparison with the one obtained by using the first 11 Fourier components, S_n, derived by the analytical expression. Fairly good agreement is observed, which confirms that the period of the THz modulation $T_{\mathrm{mod}} = 2\pi/\omega_{\mathrm{mod}}$ is no longer dependent on the frequency of the mechanical resonator; in principle, arbitrary fast signals can be sampled. Furthermore, high mechanical quality factors Q can be very beneficial, as the mechanical response at resonance is proportional to Q. As shown above, it is sufficient to scan in a frequency interval $\sim\omega_0/Q$ around each Fourier peak at $\omega_{\mathrm{sweep}} = n\omega_{\mathrm{mod}} + \omega_0$, and the experimental procedure can, thus, be optimized.

In conclusion, we have demonstrated two methods for sampling the Fourier components of a periodic signal imprinted on a Terahertz carrier. Both methods use a mechanical nanocantilever as an efficient bandpass filter, in which the very high-quality factor achievable in such systems becomes an important asset for the detection of the Fourier harmonics. When our device is combined with an external amplitude modulator, signals with arbitrary periods can be sampled. These methods are not restricted to a particular domain of the electromagnetic spectrum and are not bound to a specific material platform for the realization of the device. Specifically, for the THz range, several

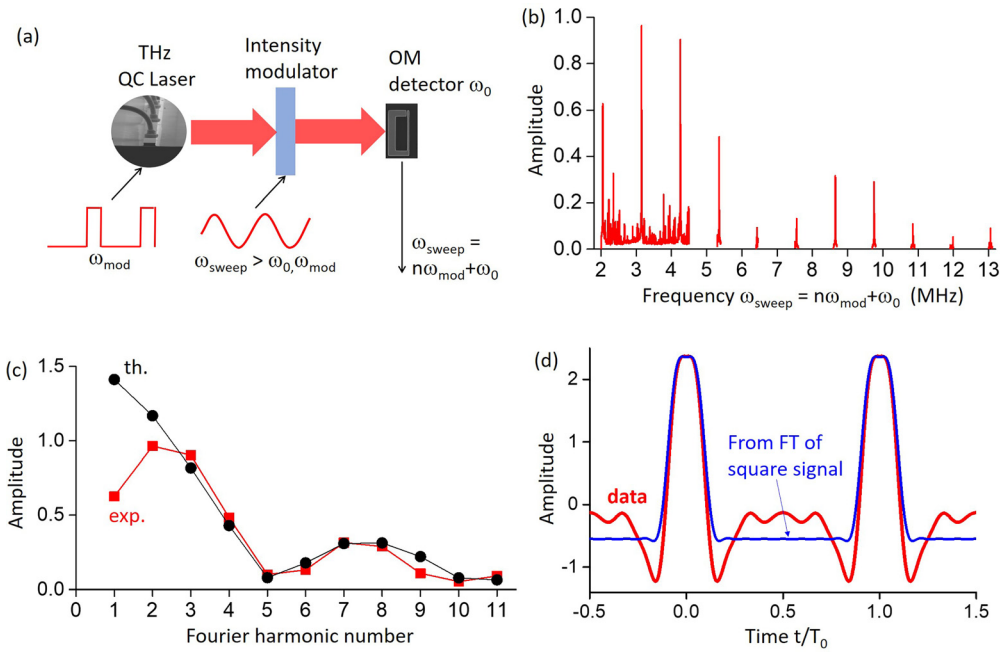

FIG. 5. (a) Outline of an experimental procedure that allows measuring the Fourier components of a THz envelope with a fixed modulation frequency. The THz signal is passed through an intensity modulator that overmodulates the signal with a variable frequency ω_{sweep}. The output signal contains harmonics with a frequency $\omega_{sweep} - n\omega_{mod}$ that can be matched with the frequency of the opto-mechanical (OM) detector ω_0. (b) Experimental implementation, where a square wave with a frequency ω_m is multiplied by a cosine signal with a variable frequency ω_{sweep}. This combined signal is written in the driving current of the THz laser. The graph shows the signal recorded on the OM detector as a function of ω_{sweep}. (c) Amplitude of the peaks from (b) as a function of the peak index. (d) Temporal reconstruction of the square wave signal and comparison with analytical results using the same number of Fourier components as the data.

types of modulators have been demonstrated so far.[18] For the typical frequency of operation of the QCL, a possible technology is modulators based on unipolar devices,[19] which can have cutoff frequencies on the order of 10 GHz.[20] On the other hand, nano-mechanical resonators with resonant frequencies up to 2 GHz have already been demonstrated.[21] Therefore, signals with frequencies on the order of 100 MHz–1 GHz could be sampled with our method.

We acknowledge device fabrication by Cherif Belacel, as well as financial support from the ANR-18-CE24-0025 project TIGER and the ENS-Thales Chair.

AUTHOR DECLARATIONS

Conflict of Interest

The authors have no conflicts to disclose.

DATA AVAILABILITY

The data that support the findings of this study are available within the article.

REFERENCES

[1]M. Tonouchi, Nat. Photonics **1**, 97–105 (2007).
[2]S. S. Dhillon *et al.*, J. Phys. D: Appl. Phys. **50**, 043001 (2017).
[3]J. L. Coutaz, *Optoélectronique Terahertz* (EDP edition, Paris, 2017).
[4]R. A. Lewis, J. Phys. D: Appl. Phys. **52**, 433001 (2019).
[5]M. Jeannin, T. Bonazzi, D. Gacemi *et al.*, Appl. Phys. Lett. **117**, 251102 (2020).
[6]H. Luo, H. C. Liu, C. Y. Song *et al.*, Appl. Phys. Lett. **86**, 231103 (2005).
[7]R. Hussin, Y. Chen, and Y. Luo, IEEE Trans. Electron Devices **63**, 3971–3976 (2016).
[8]M. S. Vitiello, D. Coquillat, L. Viti *et al.*, Nano Lett. **12**, 96–101 (2012).
[9]Y. Li, K. Tantiwanichapan, A. K. Swan, and R. Paiella, Nanophotonics **9**(7), 1901–1920 (2020).
[10]C. Belacel, Y. Todorov, S. Barbieri *et al.*, Nat. Commun. **8**, 1578 (2017).
[11]Y. Zhang, S. Hosono, N. Nagai *et al.*, J. Appl. Phys. **125**, 151602 (2019).
[12]F. Alves, D. Grbovic, B. Kearney *et al.*, Opt. Lett. **37**, 1886 (2012).
[13]A. Calabrese, D. Gacemi, M. Jeannin *et al.*, Nanophotonics **8**(12), 2269 (2019).
[14]J. H. Scofield, Am. J. Phys. **62**(2), 129–133 (1994).
[15]C. Metzger, I. Favero, A. Ortlieb *et al.*, Phys. Rev. B **78**, 035309 (2008).
[16]P. Paolino, B. Tiribilli, and L. Bellon, J. Appl. Phys. **106**, 094313 (2009).
[17]R. Hamming, *Numerical Methods for Scientists and Engineers* (Dover Publications, 1987).
[18]Z. T. Ma, Z. X. Geng, Z. Y. Fan *et al.*, Research **2019**, 6482975.
[19]*Intersubband Transitions in Quantum Wells, Physics and Device Applications*, I & II, Semiconductors and Semimetals Vols. 62 and 66, edited by H. C. Liu and F. Capasso (Academic Press, 1999).
[20]H. Dely, T. Bonazzi, O. Spitz *et al.*, "Unipolar quantum optoelectronics for high-bitrate data transmission," arXiv:2110.06572.
[21]I. Ghorbel, F. Swiadek, R. Zhu *et al.*, APL Photonics **4**, 116103 (2019).